DYNAMIC ANALYSIS OF PLANAR FLEXIBLE MECHANISMS

A Thesis Submitted to
the Graduate School of Engineering and Sciences of
İzmir Institute of Technology
in Partial Fulfillment of the Requirements for the Degree of

MASTER OF SCIENCE

in Mechanical Engineering

by
Duygu ÇÖMEN

July 2011
İZMİR

We approve the thesis of **Duygu ÇÖMEN**

Assoc. Prof. Dr. Bülent YARDIMOĞLU
Supervisor

Assist. Prof. Dr. M. İ. Can DEDE
Committee Member

Assist. Prof. Dr. Levent MALGACA
Committee Member

07 July 2011

Prof. Dr. Metin TANOĞLU
Head of the Department of
Mechanical Engineering

Prof. Dr. Durmuş Ali DEMİR
Dean of the Graduate School
of Engineering and Sciences

ACKNOWLEDGEMENTS

First, before all else, I would like to thank to my thesis advisor Assoc. Prof. Dr. Bülent Yardımoğlu for the valuable advice and support that he has given me during my thesis writing task and during my position as a research assistant at Izmir Institute of Technology.

I am sincerely grateful to faculty members and colleagues at the Department of Mechanical Engineering. My special thanks go to my family who supported and encouraged me to complete this task.

ABSTRACT

DYNAMIC ANALYSIS OF PLANAR FLEXIBLE MECHANISMS

In this study, dynamic behaviors of planar mechanisms with elastic linkages are investigated. For this purpose, slider-crank mechanisms which are widely used in many fields of industry are chosen. Flexible coupler of the mechanism is considered as a pin jointed beam under the effect of elastic oscillations in transverse direction. Euler-Bernoulli beam theory is considered to obtain dynamic responses of the elastic link. Lumped parameters approach is used to model the flexible links. Since, the assumption of small deflections is made, linear and continuous form of the elastic curve equation is written for each lumped masses on the beam to derive the equations of motion of the system. Derived set of nonlinear partial differential equations are reduced to ordinary differential equations by applying finite difference method. Finally, a symbolic mathematical program which gives the dynamic responses of the system is developed to solve the equations of motion. The results obtained from the developed program are tested and verified by the results available in the literature. Elastic deflection results are obtained for different parameters such as mass ratio and length ratio of the links of the mechanisms. The effects of the aforementioned parameters on dynamic response are found and presented in graphical forms.

ÖZET

DÜZLEMSEL ESNEK MEKANİZMALARIN DİNAMİK ANALİZİ

Bu çalışmada, elastik uzuvlu düzlemsel mekanizmaların dinamik davranışları incelenmiştir. Bu amaçla, birçok sanayi alanında sıklıkla kullanılan krank-biyel mekanizmaları seçilmiştir. Mekanizmanın esnek biyel uzvu, enine titreşimlerin etkisi altında pimler ile mesnetlenmiş bir çubuk olarak ele alınmıştır. Elastik uzvun dinamik cevaplarını elde etmek için Euler-Bernoulli çubuk teorisi uygulanmıştır. Esnek çubuğu modellemek için topaklanmış kütleler yöntemi kullanılmıştır. Küçük yerdeğiştirmeler kabulü yapıldığından, sistemin hareket denklemlerini elde etmek için elastik eğri denkleminin lineer ve sürekli hali, çubuk üzerindeki her bir topaklanmış kütle için yazılmıştır. Elde edilen nonlineer ve kısmi diferansiyel denklem takımı, sonlu farklar yöntemi uygulanarak adi diferansiyel denklem takımına dönüştürülmüştür. Son olarak, sistemin dinamik cevaplarını veren hareket denklemlerini çözmek için sembolik bir matematiksel program geliştirilmiştir. Geliştirilen programdan elde edilen sonuçlar, literatürdeki mevcut sonuçlarla karşılaştırılmış ve doğruluğu sağlanmıştır. Mekanizmaya ait kütle oranı, uzuv boy oranı gibi farklı parametreler için elastik yerdeğiştirme sonuçları elde edilmiştir. Bahsedilen parametrelerin dinamik cevaplara etkileri bulunmuş ve grafikler halinde sunulmuştur.

TABLE OF CONTENTS

LIST OF FIGURES

Figure **Page**

LIST OF SYMBOLS

A	cross-sectional area
$\vec{a}_i$	acceleration vector of point *i*
$\vec{a}_{xi}$	*x* component of acceleration vector of point *i*
$\vec{a}_{yi}$	*y* component of acceleration vector of point *i*
a_{G2x}	*x* component of acceleration of the center of mass for crank
a_{G2y}	*y* component of acceleration of the center of mass for crank
a_{G3x}	*x* component of acceleration of the center of mass for coupler
a_{G3y}	*y* component of acceleration of the center of mass for coupler
$a_x(x,t)$	function of *x* component of the acceleration
$a_y(x,t)$	function of *y* component of the acceleration
b	width of the cross-section of the coupler
$\vec{D}_{xi}$	*x* component of D'Alembert force acting on mass *i*
$\vec{D}_{yi}$	*y* component of D'Alembert force acting on mass *i*
E	modulus of elasticity
$\vec{F}^{\,i}$	inertial force
F_x^{23}	*x* component of the joint force exerted on link 3 by link 2
F_y^{23}	*y* component of the joint force exerted on link 3 by link 2
F_X^{43}	*x* component of the joint force exerted on link 3 by link 4 in terms of global coordinate system
F_Y^{43}	*y* component of the joint force exerted on link 3 by link 4 in terms of global coordinate system
F_x^{43}	*x* component of the joint force exerted on link 3 by link 4 in terms of local coordinate system
F_y^{43}	*y* component of the joint force exerted on link 3 by link4 in terms of local coordinate system
g_2	relative position of mass center of crank

g_3	relative position of mass center of coupler
h	height of the cross-section of the coupler
I	second moment of area
i	notation of an arbitrary point
$\vec{i}$	unit vector in x direction
$\vec{j}$	unit vector in y direction
$\vec{k}$	unit vector in z direction
l	distance parameter used between lumped masses
L_2	length of the crank
L_3	length of the coupler
m_{3i}	mass of the i-th lumped mass on coupler
M_2	mass of link 2
M_3	mass of link 3
M_4	mass of link 4
$M(x,t)$	bending moment along the coupler
n	number of lumped masses
$\vec{\mathrm{r}}$	position vector of origin of the local coordinate frame
$\vec{r}_i$	position vector of point i
s_4	position of the slider
$\vec{s}_i$	position vector of point i with respect to local coordinate system
$\vec{s}_{xi}$	x component of the vector $\vec{s}_i$
$\vec{s}_{yi}$	y component of the vector $\vec{s}_i$
$S(x,t)$	shear force along the coupler
$\vec{u}_i$	elastic deflection vector
$\vec{u}_{xi}$	x component of elastic deflection vector
$\vec{u}_{yi}$	y component elastic deflection vector
$\vec{v}_i$	velocity of point i
$v(x,t)$	elastic transverse deflection of coupler
x_i	position of mass i on coupler

$\vec{\alpha}$	angular acceleration vector
α_2	angular acceleration of crank
α_3	angular acceleration of coupler
Δx	mesh size on x domain
θ	angle between global and local coordinate frames
θ_2	crank angle measured from the X axis
θ_3	coupler angle measured from the X axis
ξ	independent variable for position
ρ	density
ω	angular velocity
ω_2	angular velocity of crank
ω_3	angular velocity of coupler
$\dot{(\ )}$	derivative with respect to "t"

CHAPTER 1

INTRODUCTION

Dynamic analysis of flexible mechanisms is one of the significant problems in engineering research areas. By developments in robot technologies, utilization of various mechanisms in many fields of industry is increased. Most of mechanisms are designed to minimize the vibrations and maximize the stiffness of the mechanism components; however this design purposes make the mechanisms heavy. The usage of high weighted mechanisms is not convenient in many fields of engineering and industrial applications.

The weight of the components of robot manipulators, mechanisms and machines is one of the important design restrictions. Furthermore, high operation speeds, good efficiency, low manufacturing costs and so forth, are other design criteria that engineers take into account in modern machinery. The quest for these design features requires to use low weighted and slender components for various mechanisms, robot manipulators and machines. Namely, reducing the weight of the mechanisms is necessary for increasing accurate performance, having superior efficiency and decreasing energy consumption in modern machinery.

On the other hand, there are disadvantages that appear on the light weighted and high operated systems. Because of the high operation speeds and the slenderness of the components of mechanisms, elastic oscillations may occur. It is clear that, due to these elastic oscillations, classical rigid body model gives ineffective solutions in dynamic analysis of the components of mechanisms. So, these components must be thought as flexible and a new model that takes into account this flexibility feature must be used in modelling and analyzing flexible mechanisms.

Mechanisms with high operation speeds and light weighted, slender components are considered as flexible multibody systems. Planar mechanisms, like slider-crank mechanisms and four-bar mechanisms which serve as a model of flexible multibody systems are widely used in industry.

Along with technological developments, many researchers have been investigated modeling, dynamic analysis and control of flexible mechanisms since 1970s.

Different types of approaches to derive the mathematical model and equations of motion of flexible mechanisms are used by the researchers. Beside, different solution techniques for derived equations of motion are investigated. The significant examples of those studies are summarized to clarify the main theme of the flexible mechanism investigations.

Vibration and stress analysis of a slider-crank mechanism with rigid crank and flexible coupler is given. A lumped parameter approach is derived to obtain elastic deflections of moving linkages. Euler-Bernoulli beam theory is applied to the system to obtain equations of motion (Sadler and Sandor 1973). A similar study is done to analyze planar four-bar mechanism. Lumped parameter approach is applied to have dynamic response of three links of moving mechanism (Sadler and Sandor 1974). Those studies are improved to give stress-strain responses together with elastic deflections of linkages in a four-bar mechanism (Sadler and Sandor 1975). The bending vibration of an elastic connecting rod in a slider-crank mechanism is investigated. Energy methods are used to derive the equations of motion. Derived partial differential equations are converted to ordinary differential equations by application of Galerkin variational technique and dynamic responses of elastic coupler are given (Viscomi and Ayre 1971). Free vibration analysis of planar four-bar mechanisms is presented by using finite element method. Higher-order beam elements are employed to each flexible link for axial and lateral elastic deformations. Dynamical frequencies and dynamical mode shapes taking into account gyroscopic effects and dynamical axial loads are obtained (Yu and Xi 2003). Vibration control of a four-bar mechanism with a flexible coupler is investigated. The fully coupled nonlinear equations of motion are derived using Lagrangian approach (Karkoub and Yigit 1999). Dynamical stabilities of slider-crank and four-bar mechanisms with flexible coupler are studied. Elastic coupler is considered as Euler-Bernoulli beam (Turhan 1993). A method for dynamic stability analysis of a closed-loop flexible mechanism by using modal coordinates is presented (Yang and Park 1998). Dynamic instability of high-speed flexible four-bar mechanisms is investigated. Equations of motion for global system are formulated using Lagrange equations and finite element method is employed to model each unconstrained flexible links (Yu and Cleghorn 2002). An expression for the equations of motion of flexible multibody

systems with rigid and flexible components are developed using Lagrangian approach (Fanghella et al. 2003). Time dependent boundary effect on the dynamic responses of the flexible connecting rod of a slider-crank mechanism is studied (Fung 1997). Furthermore, dynamical behavior of a damped flexible connecting rod with the effects of rigid crank length is investigated (Chen and Chian 2001). Kinematics and kinetics of mechanisms are given (Söylemez 1999). Rigid and flexible multibody motions and mechanics of deformable bodies are introduced (Shabana 2005). Dynamics of flexible multibody systems are given. (de Jalon and Bayo 1993).

Flexible mechanisms have been subjected to various investigations ever since the first studies were given in 1970s. However, to our best knowledge, if the wide usage of flexible mechanisms in modern industry is taken into account, it is seen that there is not enough study and application on this issue. Therefore, in this study, dynamic behavior of flexible linkages in slider-crank mechanisms is investigated. Elastic deflections of the flexible links are determined and the effects of various parameters on the dynamic behavior are discussed. Euler-Bernoulli beam theory is used to derive the equations of motion and Finite Difference schemes are applied to non-linear partial differential equations of motion.

In Chapter 2, rigid and flexible body motions are introduced briefly. Kinematic and kinetic analyses of planar slider-crank mechanism are given for both rigid mechanism and mechanism with flexible coupler. Finite Difference Method for elastic deflections is presented. Applications and numerical examples for slider-crank mechanisms having flexible coupler are given in Chapter 3. Lastly, conclusions are given in Chapter 4.

CHAPTER 2

ANALYSIS OF PLANAR MECHANISMS

2.1. Rigid Slider-Crank Mechanism

2.1.1. Rigid Body Motion

The configuration of a point on a rigid body can be expressed through local and fixed coordinate systems. As the position and orientation of the fixed coordinate system never change with time, local coordinate system whose origin is attached to the body moves with the rigid body. In Figure 2.1, an arbitrary point *i* on a rigid body is shown and the position of the point in terms of fixed coordinate system can be written as follows (Shabana 2005):

$$\vec{r}_i = \vec{r} + \vec{s}_i \tag{2.1}$$

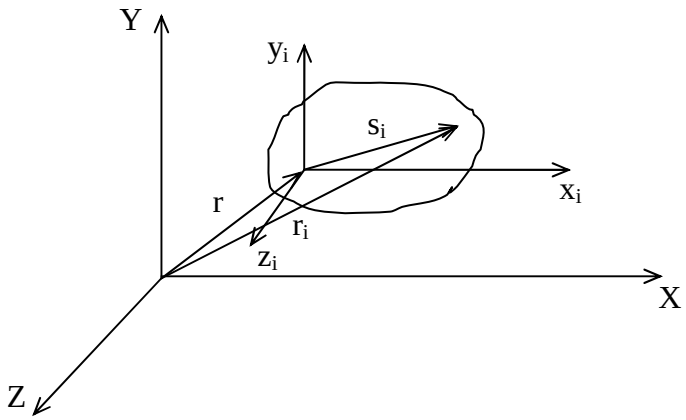

Figure 2.1. References of a rigid body

Furthermore, in terms of local coordinate system which attached to the rigid body, point *i* can be expressed as follows, where $\vec{i}$ and $\vec{j}$ are the unit vectors belong to local coordinate system:

$$\vec{s}_i = s_{xi}\vec{i} + s_{yi}\vec{j} \tag{2.2}$$

To obtain the velocity expressions of point *i*, it is required to derivate the position equations with respect to time. It is obvious that s_{xi} and s_{yi} are constant.

$$\vec{v}_i = \frac{d\vec{r}_i}{dt} = \dot{\vec{r}} + \dot{\vec{s}}_i \tag{2.3}$$

Differentiation of the vector $\vec{s}_i$ is found by considering the time derivatives of unit vectors $\vec{i}$ and $\vec{j}$ which are given as $\dot{\vec{i}} = \dot{\theta}_3\vec{j}$ and $\dot{\vec{j}} = -\dot{\theta}_3\vec{i}$, respectively.

$$\dot{\vec{s}}_i = s_{xi}\frac{d\vec{i}}{dt} + s_{yi}\frac{d\vec{j}}{dt} = s_{xi}\dot{\theta}\vec{j} - s_{yi}\dot{\theta}\vec{i} \tag{2.4}$$

where θ is rotation angle of the local coordinate system.

An angular velocity of rigid body is introduced as the time derivative of angle θ:

$$\vec{\omega} = \dot{\theta}\vec{k} \tag{2.5}$$

Equation 2.4 can be written as:

$$\dot{\vec{s}}_i = \vec{\omega} \times \vec{s}_i \tag{2.6}$$

Substituting Equation 2.6 to Equation 2.3, velocity expression for point *i* in terms of fixed coordinate system is obtained as:

$$\vec{v}_i = \dot{\vec{r}}_i + \vec{\omega} \times \vec{s}_i \tag{2.7}$$

Furthermore, acceleration expressions which consist of coordinates and their time derivatives can be obtained by differentiation with respect to time:

$$\vec{a}_i = \ddot{\vec{r}}_i + \dot{\vec{\omega}} \times \vec{s}_i + \vec{\omega} \times \dot{\vec{s}}_i \tag{2.8}$$

An angular acceleration is defined as second derivative of angle θ:

$$\vec{\alpha} = \ddot{\theta}\,\vec{k} \tag{2.9}$$

And Equation 2.8 can be rewritten as:

$$\vec{a}_i = \ddot{\vec{r}}_i + \vec{\alpha} \times \vec{s}_i + \vec{\omega} \times \vec{\omega} \times \vec{s}_i \tag{2.10}$$

2.1.2. Kinematics of Rigid Slider-Crank Mechanism

Position, velocity and acceleration expressions of a rigid slider-crank mechanism are given in this section. In Figure 2.2, a sample mechanism with the names of the components is shown.

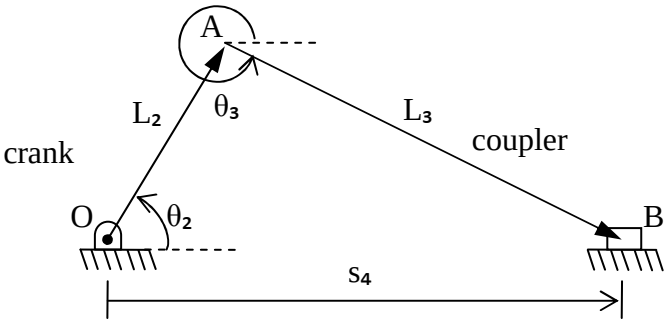

Figure 2.2. Slider-crank mechanism

When the crank angle θ_2 is taken as input of the system, a vector loop equation can be written as follows (Söylemez 1999):

$$\vec{L}_2 + \vec{L}_3 = \vec{s}_4 \tag{2.11}$$

It should be noted that the vector s_4 varies with the position of the slider, therefore the magnitude of the vector s_4 is unknown. Equation 2.11 can be written considering the magnitudes and directions of vectors as:

$$L_2 \cos\theta_2 \, \vec{i} + L_2 \sin\theta_2 \, \vec{j} + L_3 \cos\theta_3 \, \vec{i} + L_3 \sin\theta_3 \, \vec{j} = s_4 \, \vec{i} \tag{2.11}$$

Equation 2.11 can be resolved into horizontal and vertical components as:

$$L_2 \cos\theta_2 + L_3 \cos\theta_3 = s_4 \tag{2.12}$$

$$L_2 \sin\theta_2 + L_3 \sin\theta_3 = 0 \tag{2.13}$$

Considering the input crank angle θ_2 is known, the unknown angle θ_3 belong the position analysis of slider-crank mechanism can be obtained as:

$$\theta_3 = Arc\sin\left(-\frac{L_2}{L_3} \sin\theta_2 \right) \tag{2.14}$$

It should be noted that, Equation 2.12 gives the position of the slider with respect to global coordinate system.

In order to make velocity analysis, differentiations with respect to time of the loop closure equation for horizontal and vertical components should be written:

$$-L_2 \omega_2 \sin\theta_2 - L_3 \omega_3 \sin\theta_3 = \dot{s}_4 \tag{2.15}$$

$$L_2 \omega_2 \cos\theta_2 + L_3 \omega_3 \sin\theta_3 = 0 \tag{2.16}$$

where the angular velocities ω_2 and ω_3 are:

$$\omega_2 = \dot{\theta}_2 = \frac{d\theta_2}{dt} \tag{2.17}$$

and

$$\omega_3 = \dot{\theta}_3 = \frac{d\theta_3}{dt} \tag{2.18}$$

Angular velocity of the crank is known and by arranging Equations 2.15 and 2.16, unknown parameters for velocity analysis are found as:

$$\omega_3 = -\frac{L_2 \cos\theta_2}{L_3 \cos\theta_3}\omega_2 \tag{2.19}$$

and velocity of the slider with respect to point *O* is:

$$\dot{s}_4 = L_2 \frac{\sin(\theta_2 - \theta_3)}{\cos(\theta_3)}\omega_2 \tag{2.20}$$

Lastly, time derivatives of the velocity loop equation are taken to obtain acceleration loop equations:

$$-L_2 \alpha_2 \sin\theta_2 - L_2 \omega_2^{\,2} \cos\theta_2 - L_3 \alpha_3 \sin\theta_3 - L_3 \omega_3^{\,2} \cos\theta_3 = \ddot{s}_4 \tag{2.21}$$

$$L_2 \alpha_2 \cos\theta_2 - L_2 \omega_2^{\,2} \sin\theta_2 + L_3 \alpha_3 \cos\theta_3 - L_3 \omega_3^{\,2} \sin\theta_3 = 0 \tag{2.22}$$

where the angular accelerations are defined as time derivatives of the angular velocities:

$$\alpha_2 = \dot{\omega}_2 = \frac{d\omega_2}{dt} \tag{2.23}$$

and

$$\alpha_3 = \dot{\omega}_3 = \frac{d\omega_3}{dt} \tag{2.24}$$

Equations 2.21 and 2.22 are two equations with two unknowns, which are α_3 and $\ddot{s}_4$. By solving the aforementioned unknowns the following equations are obtained:

$$\alpha_3 = \frac{\left(L_2\,\omega_2^{\,2}\sin\theta_2 - L_2\,\alpha_2\cos\theta_2 + L_3\omega_3^{\,2}\sin\theta_3\right)}{L_3\cos\theta_3} \tag{2.25}$$

and

$$\ddot{s}_4 = -L_2\,\alpha_2\sin\theta_2 - L_2\,\omega_2^{\,2}\cos\theta_2 - L_3\,\alpha_3\sin\theta_3 - L_3\,\omega_3^{\,2}\cos\theta_3 \tag{2.26}$$

2.1.3. Kinetics of Rigid Slider-Crank Mechanism

Kinetic analysis of rigid slider-crank mechanism based on lumped mass approach requires to obtain the joint forces due to the inertia forces acting on the mass centers of the linkages.

Inertial force acting on a rigid body can be written by D'Alembert principle as:

$$\vec{F}^{\,i} = -m\vec{a}_G \tag{2.27}$$

where the vector $\vec{a}_G$ is the acceleration expression for center of gravity of the linkage.

In a slider-crank mechanism, accelerations of the mass centers of the crank and coupler can be written by using kinematic relationships of crank and couplers as follows (Söylemez 1999):

$$\mathrm{a}_{\mathrm{G2x}} = -g_2\omega_2^{\,2}\cos\theta_2 - \mathrm{g}_2\alpha_2\sin\theta_2 \tag{2.28}$$

$$\mathrm{a}_{\mathrm{G2y}} = -g_2\omega_2^{\,2}\sin\theta_2 + \mathrm{g}_2\alpha_2\cos\theta_2 \tag{2.29}$$

$$\mathrm{a}_{\mathrm{G3x}} = -\mathrm{L}_2\omega_2^{\,2}\cos\theta_2 - \mathrm{L}_2\alpha_2\sin\theta_2 - g_3\omega_3^{\,2}\cos\theta_3 - \mathrm{g}_3\alpha_3\sin\theta_3 \tag{2.30}$$

$$\mathrm{a}_{\mathrm{G3y}} = -\mathrm{L}_2\omega_2^{\,2}\sin\theta_2 + \mathrm{L}_2\alpha_2\cos\theta_2 - g_3\omega_3^{\,2}\sin\theta_3 + \mathrm{g}_3\alpha_3\cos\theta_3 \tag{2.31}$$

In Equations 2.28 to 2.31, g_2 and g_3 represent the relative positions of crank and coupler, respectively.

2.2. Flexible Slider-Crank Mechanism

2.2.1. Flexible Body Motion

According to rigid body assumption, it is considered that a body consists of a great number of particles. So, kinematic and kinetic analyses perform due to this fact. The distance between two points in a rigid body is assumed constant during the motion and a coordinate system whose origin fixed to the rigid body is adequate to define the position of any arbitrary point on the rigid body. A global and a local coordinate system which define the position and orientation of the body are simply enough to specify all of the points of the body during the motion.

However, when flexible body motion is taken into account, it is not accurate to approve the invariability of the distance between two points on a body. Due to the elastic oscillations, the positions of the points will be changed and elastic deflections will be in question during the motion. The position of an arbitrary point on the flexible body is shown in Figure 2.3. The vector $\vec{r}$ defines the position of the origin of the local coordinate frame in terms of the global coordinate frame and the constant vector $\vec{s}_i$ defines the position of the point *i* before the elastic deflection. Lastly, an elastic deflection vector $\vec{u}_i$ is defined to give the accurate position of the point *i*. (Shabana 2005)

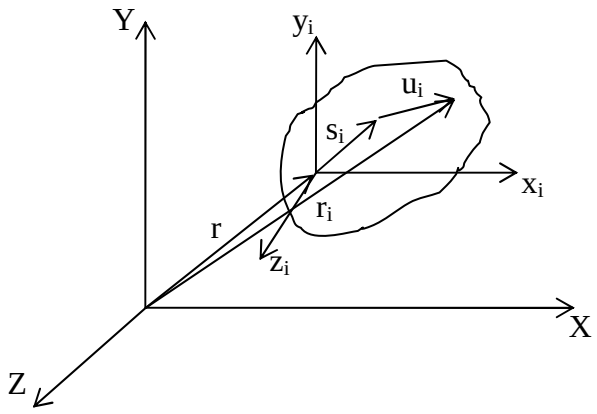

Figure 2.3. References of a flexible body

The final position of the point *i* on a flexible body with respect to global coordinate system is defined as the vector $\vec{r}_i$ and it is written as follows:

$$\vec{r}_i = \vec{r} + \vec{s}_i + \vec{u}_i \tag{2.32}$$

The vector $\vec{s}_i$ which specifies the undeformed position of point *i* is constant with respect to local coordinate system during the motion; however the vector $\vec{u}_i$ which defines the elastic deflection of the point *i* varies with time and space. As a result of this property, the equations of motion appear as partial differential equations depending on time and space.

Consequently, infinite numbers of local coordinate systems are required to give analytical solutions to flexible body motion. So, numerical methods like finite element method and finite difference method are used to achieve difficulties of solutions.

The components of undeformed position vector $\vec{s}_i$ and elastic deflection vector $\vec{u}_i$ can be expressed as:

$$\vec{s}_i = s_{xi}\vec{i} + s_{yi}\vec{j} \tag{2.33}$$

$$\vec{u}_i = u_{xi}\vec{i} + u_{yi}\vec{j} \tag{2.34}$$

It is obvious that while the components of undeformed position vector are constant during the motion with respect to local coordinate frame, the components of elastic deflection vector varies with time and space. To obtain the velocity expressions, derivations of position vectors are given below:

$$\dot{\vec{s}}_i = s_{xi}\frac{d\vec{i}}{dt} + s_{yi}\frac{d\vec{j}}{dt} = s_{xi}\dot{\theta}\,\vec{j} - s_{yi}\dot{\theta}\vec{i} \tag{2.35}$$

$$\dot{\vec{u}}_i = u_{xi}\frac{d\vec{i}}{dt} + \dot{u}_{xi}\vec{i} + u_{yi}\frac{d\vec{j}}{dt} + \dot{u}_{yi}\vec{j} = u_{xi}\dot{\theta}\,\vec{j} + \dot{u}_{xi}\vec{i} - u_{yi}\dot{\theta}\vec{i} + \dot{u}_{yi}\vec{j} \tag{2.36}$$

Time derivatives of $\vec{s}_i$ and $\vec{u}_i$ can be rewritten as:

$$\dot{\vec{s}}_i = \vec{\omega} \times \vec{s}_i \tag{2.37}$$

$$\dot{\vec{u}}_i = \vec{\omega} \times \vec{u}_i + \dot{u}_{xi}\vec{i} + \dot{u}_{yi}\vec{j} \tag{2.38}$$

where $\vec{\omega}$ is the angular velocity vector:

$$\vec{\omega} = \dot{\theta}\vec{k} \tag{2.39}$$

Finally, velocity expression for an arbitrary point *i* on a flexible body with respect to global coordinate system is given as:

$$\vec{v}_i = \dot{\vec{r}} + \vec{\omega} \times (\vec{s}_i + \vec{u}_i) + \dot{u}_{xi}\vec{i} + \dot{u}_{yi}\vec{j} \tag{2.40}$$

Acceleration vector in terms of global coordinate system for an arbitrary point *i* on a flexible body can be obtained by differentiating velocity expression with respect to time (Shabana 2005):

$$\vec{a}_i = \ddot{\vec{r}} + \vec{\omega} \times (\vec{\omega} \times (\vec{s}_i + \vec{u}_i)) + \vec{\alpha} \times (\vec{s}_i + \vec{u}_i) + 2\vec{\omega} \times (\dot{u}_{xi}\vec{i} + \dot{u}_{yi}\vec{j}) + \ddot{u}_{xi}\vec{i} + \ddot{u}_{yi}\vec{j} \tag{2.41}$$

where the angular acceleration is introduced as:

$$\vec{\alpha} = \ddot{\theta}\vec{k} \tag{2.42}$$

First term of the acceleration vector is acceleration of the origin of body-fixed coordinate frame with respect to global coordinate frame. Second and third terms are normal and tangential components of the acceleration vector of undeformed configuration of any point on flexible body with respect to body-fixed coordinate frame. Finally, last three terms are normal and tangential components of the acceleration vector of any arbitrary point on the flexible body which appear due to the elastic deflection

vector. First three terms of Equation 2.41 are similar with rigid body acceleration terms while last three terms defines the acceleration that comes from elastic deflection.

2.2.2. Kinematics of Flexible Slider-Crank Mechanism

Slider-crank mechanisms have been used in machinery systems since the early times. In modern machinery, slider-crank mechanisms are often used in many fields of engineering. A mechanism shown in Figure 2.2 is investigated in this study by flexible body motion.

In this subsection, kinematic analysis of a slider-crank mechanism is given. The connecting rod of the mechanism is considered as flexible, however the crank is assumed rigid. It can be said that, due to the short length of the crank compared to the coupler, rigid assumption will give effective and convincing solutions. Longitudinal elastic displacement of flexible coupler is neglected compared to the elastic deflections.

Global and local coordinate systems of slider-crank mechanism are shown in Figure 2.4. Global coordinate system is fixed to the origin of the rigid crank, while the origin of the local coordinate system is attached to the connecting point of the crank and couplers. The vectors $\vec{i}$ and $\vec{j}$ are the unit vectors of this local coordinate system.

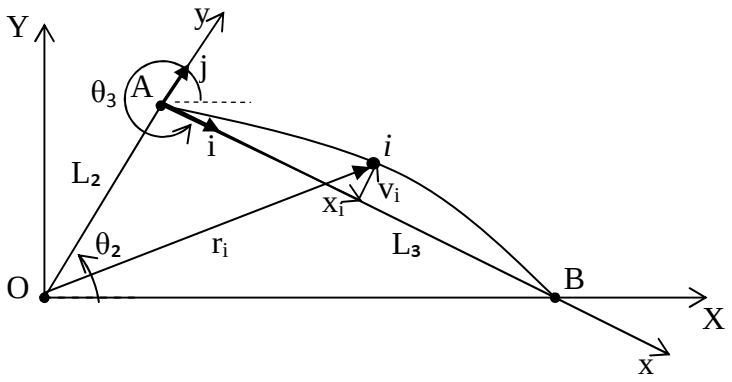

Figure 2.4. Deformed and undeformed configurations of slider-crank mechanism

Deformed and undeformed configurations of coupler are shown in the Figure 2.4. An elastic deformation function $v(x,t)$ is introduced which depends on space and mechanism configuration that varies with time. As longitudinal displacements are

neglected, function $v(x,t)$ which depend on space and time represent a deformation vector on y direction in terms of local coordinate system.

Position vector of an arbitrary point i on the flexible coupler is represented by the vector $\vec{r}_i$.

$$\vec{r}_i = (X\cos\theta_3 + Y\sin\theta_3 + x_i)\vec{i} + (Y\cos\theta_3 - X\sin\theta_3 + v_i(x,t))\vec{j} \qquad (2.43.a)$$

where X and Y are components of crank vector and written as:

$$X = L_2\cos\theta_2 \qquad (2.43.b)$$

$$Y = L_2\sin\theta_2 \qquad (2.43.c)$$

In above equation, L_2 is the length of crank, x_i is the relative position of point i before deformation, measured from the origin of the local coordinate system, θ_2 and θ_3 are the position angles of crank and couplers, respectively.

Noting that the derivations of $\vec{\mathrm{i}}$ and $\vec{\mathrm{j}}$ are $\dot{\vec{\mathrm{i}}} = \dot{\theta}_3\vec{j}$ and $\dot{\vec{\mathrm{j}}} = -\dot{\theta}_3\vec{i}$, the velocity vector of arbitrary point i can be obtained by derivation of Equation 2.43 with respect to time:

$$\begin{aligned}\vec{v}_i = {} & (-L_2\dot{\theta}_2\sin\theta_2\cos\theta_3 + L_2\dot{\theta}_2\cos\theta_2\sin\theta_3 - \dot{\theta}_3 v_i(x,t))\vec{i} \\ & + (L_2\dot{\theta}_2\sin\theta_2\sin\theta_3 + L_2\dot{\theta}_2\cos\theta_2\cos\theta_3 + \dot{v}_i(x,t) + \dot{\theta}_3 x_i)\vec{j}\end{aligned} \qquad (2.44)$$

Finally, time derivation of velocity vector is given below as the acceleration expression of an arbitrary point on deformable coupler in slider-crank mechanism.

$$\begin{aligned}\vec{a}_i = {} & (-L_2\ddot{\theta}_2\sin\theta_2\cos\theta_3 - L_2\dot{\theta}_2^{\,2}\cos\theta_2\cos\theta_3 + L_2\ddot{\theta}_2\cos\theta_2\sin\theta_3 - L_2\dot{\theta}_2^{\,2}\sin\theta_2\sin\theta_3 \\ & - x_i\dot{\theta}_3^{\,2} - 2\dot{\theta}_3\dot{v}_i(x,t) - \ddot{\theta}_3 v_i(x,t))\vec{i} + (L_2\ddot{\theta}_2\sin\theta_2\sin\theta_3 + L_2\dot{\theta}_2^{\,2}\cos\theta_2\sin\theta_3 \\ & + L_2\ddot{\theta}_2\cos\theta_2\cos\theta_3 - L_2\dot{\theta}_2^{\,2}\sin\theta_2\cos\theta_3 + x_i\ddot{\theta}_3 + \ddot{v}_i(x,t) - \dot{\theta}_3^{\,2}v_i(x,t))\vec{j}\end{aligned} \qquad (2.45)$$

For the constant angular velocity of the crank, longitudinal and transverse components of acceleration vectors become:

$$\vec{a}_{xi} = -L_2\dot{\theta}_2^{\,2}\cos\theta_2\cos\theta_3 - L_2\dot{\theta}_2^{\,2}\sin\theta_2\sin\theta_3 - x_i\dot{\theta}_3^{\,2} - 2\dot{\theta}_3\dot{v}_i(x,t) - \ddot{\theta}_3 v_i(x,t) \quad (2.46)$$

$$\vec{a}_{yi} = L_2\dot{\theta}_2^{\,2}\cos\theta_2\sin\theta_3 - L_2\dot{\theta}_2^{\,2}\sin\theta_2\cos\theta_3 + x_i\ddot{\theta}_3 + \ddot{v}_i(x,t) - \dot{\theta}_3^{\,2} v_i(x,t) \quad (2.47)$$

Because of the rigid body assumption for crank, the relation between the crank angle θ_2 and the coupler angle θ_3 can be written by using the geometrical properties as follows:

$$\theta_3 = \arcsin(-\frac{L_2}{L_3}\sin\theta_2) \quad (2.48)$$

It should be noted that, both angles θ_2 and θ_3 are depend on moving mechanism configuration that varies with time.

Consequently, the acceleration vectors in *x* and *y* direction which will be mentioned in derivation of equations of motion leads to inertia forces.

2.2.3. Kinetics of Flexible Slider-Crank Mechanism

Kinetic analysis of slider-crank mechanism with flexible coupler is given in this section. In Figure 2.5, the forces acting on the coupler are shown.

The forces F_x^{23} and F_y^{23} are *x* and *y* components of the joint forces exerted on coupler *3* by the rigid crank *2*. Similarly, the forces F_x^{43} and F_y^{43} are *x* and *y* components of the joint forces at point *B*.

D'Alembert forces acting on an arbitrary point *i* in *x* and *y* directions which are also shown in Figure 2.5 constitute the inertia forces. These forces associated with acceleration expressions in *x* and *y* directions are written as follows:

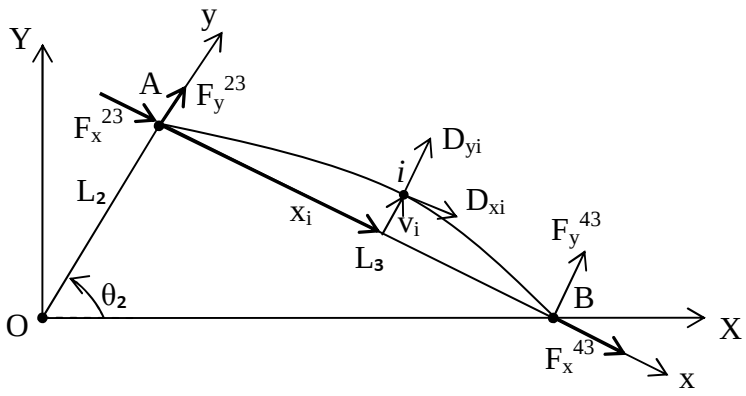

Figure 2.5. Forces acting on flexible coupler

$$\vec{D}_{xi} = -M_3 \vec{a}_{xi} \tag{2.49}$$

$$\vec{D}_{yi} = -M_3 \vec{a}_{yi} \tag{2.50}$$

The mass on point ion coupler can be considered as a differential mass; thus, D'Alembert forces can be taken into account as distributed parameter system.

Force equilibrium in longitudinal and transverse directions and moment equilibrium about origin of the local coordinate system are written to obtain joint forces in terms of inertia forces:

$$F_x^{23} + F_x^{43} + \int_0^{L_3} \rho A a_x(x,t)\, dx = 0 \tag{2.51}$$

$$F_y^{23} + F_y^{43} + \int_0^{L_3} \rho A a_y(x,t)\, dx = 0 \tag{2.52}$$

$$F_y^{43} L_3 + \int_0^{L_3} \rho A a_y(x,t)\, x\, dx - \int_0^{L_3} \rho A a_x(x,t)\, v_i(x,t)\, dx = 0 \tag{2.53}$$

where ρ is mass per unit length and A is cross-sectional area of the coupler. By, arranging these equations, transverse reaction forces can easily be found as:

$$F_y^{43} = -\frac{1}{L_3}\int_0^{L_3} \rho A a_y(x,t)\, x\, dx + \frac{1}{L_3}\int_0^{L_3} \rho A a_x(x,t) v_i(x,t)\, dx \tag{2.54}$$

$$F_y^{23} = -F_y^{43} - \int_0^{L_3} \rho A a_y(x,t)\, dx \tag{2.55}$$

To obtain the longitudinal joint forces F_x^{23} and F_x^{43}, it is necessary to consider the condition of the piston denoted by capital B shown in Figure 2.6. The forces F_X^{43} and F_Y^{43} which are written in terms of global coordinate system are components of joint force at point B. These forces are shown in Figure 2.6 clearly.

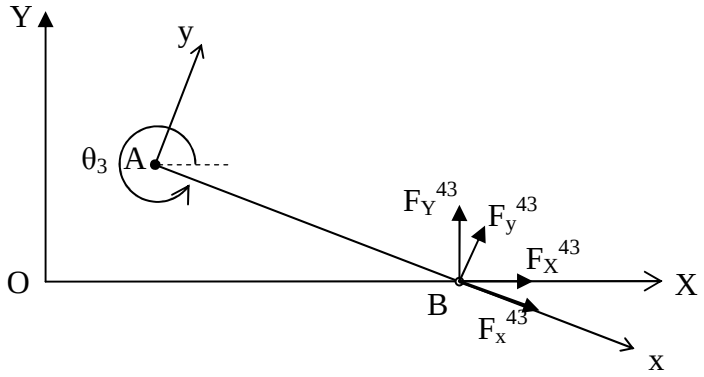

Figure 2.6. Joint forces at the end point of coupler

$$\begin{bmatrix} F_x^{43} \\ F_y^{43} \end{bmatrix} = \begin{bmatrix} \cos\theta_3 & \sin\theta_3 \\ -\sin\theta_3 & \cos\theta_3 \end{bmatrix} \begin{bmatrix} F_X^{43} \\ F_Y^{43} \end{bmatrix} \tag{2.56}$$

Equation 2.56 can be written separately as:

$$F_x^{43} = F_X^{43}\cos\theta_3 + F_Y^{43}\sin\theta_3 \tag{2.57.a}$$

$$F_y^{43} = -F_X^{43}\sin\theta_3 + F_Y^{43}\cos\theta_3 \qquad (2.57.b)$$

The relation between these joint forces are arranged to give longitudinal components which are determined as:

$$F_x^{43} = F_y^{43}\cot\theta_3 + F_X^{43}\csc\theta_3 \qquad (2.58)$$

where F_X^{43} can be found from dynamic equilibrium condition of slider:

$$F_X^{43} = -M_4(L_2\omega_2^2\cos\theta_2 + L_3\dot{\theta}_3^2\cos\theta_3 + L_3\ddot{\theta}_3\sin\theta_3) \qquad (2.59)$$

Similar to Equation 2.55:

$$F_x^{23} = -F_x^{43} - \int_0^{L_3}\rho A a_x(x,t)dx \qquad (2.60)$$

These reaction forces are effect to response of flexible coupler by bending moment expression which will be introduced in next section.

2.3. Derivation of Equations of Motion

Derivation of equations of motion for a slider-crank mechanism with flexible coupler is given in this section. Flexible link is assumed as a pin jointed beam under the effect of harmonic transverse loading.

2.3.1. Distributed Parameter Method

Dynamic response, namely elastic deflections of beam is obtained by applying Euler-Bernoulli beam theory. Small deflection assumption is made to use the linear and continuous form of the elastic curve equation given as:

$$EI\frac{\partial^2 v(x,t)}{\partial x^2} = M(x,t) \tag{2.61}$$

where E is modulus of elasticity and I is second moment of area of the cross-section of the beam.

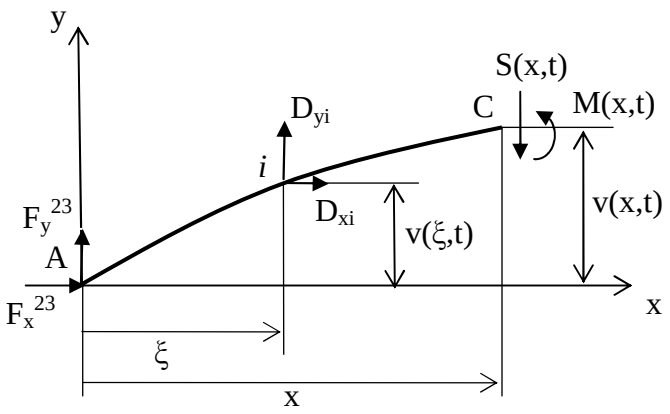

Figure 2.7. Free body diagram of the left part of the coupler

A new independent variable ξ which is shown in Figure 2.7 is introduced to obtain the integral summation of inertia forces denoted by D_{xi} and D_{yi} over the x domain. Taking the moment about point C, the following expression can be written for bending moment:

$$\begin{aligned} M(x,t) = F_y^{23}x - F_x^{23}v_i(x,t) + \int_0^x \rho A\xi\, a_y(\xi,t)\, d\xi \\ - \int_0^x \rho A(v(x,t) - v(\xi,t))\, a_x(\xi,t)\, d\xi \end{aligned} \tag{2.62}$$

Equations 2.61 and 2.62, constitute the equation of motion of the coupler. It is noted that, the forces F_y^{23} and F_x^{23} should be substituted into the equation of motion to express it explicitly. The boundary conditions which should be satisfied for a pin jointed beam are given as:

$$v(0,t)=0 \tag{2.63}$$

and

$$v(L_3,t)=0 \tag{2.64}$$

However, integro-differential equation that explained above cannot be solved by the analytical techniques because of the complexity of the equation. Therefore, a method of lumped parameter is employed to reduce the system to a more convenient form of set of differential equations (Sadler and Sandor 1973).

2.3.2. Lumped Parameter Method

Lumped parameter method can be used in vibration analysis to obtain the natural frequencies and to determine the vibration responses when the analytical solutions are not available. By using this method, the results having desired accuracy can be obtained.

In this study, lumped parameter method gives a set of differential equations instead of a single equation contains integral and differential terms by considering lumped masses instead of distributed one. A finite number of equally lumped masses are considered for flexible coupler. The sum of the lumped masses m_{3i} is equal to the total mass M_3 of the link 3.

$$M_3=\sum_{i=1}^{n} m_{3i} \tag{2.65}$$

where i is the mass number and n is the total number of the lumped masses.

In Figure 2.8, the configuration of lumped masses is shown. No masses are located on left and right boundaries of the link, since these points are the boundaries of the coupler. Otherwise, lumped masses on the boundaries would be required extra computational effort for joint force calculations.

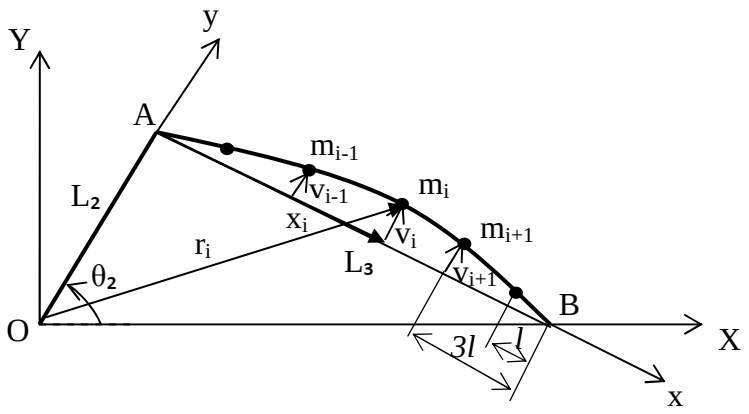

Figure 2.8. Lumped masses on flexible coupler

Lumped masses are located on the neutral axis of the beam with the distance *2l*, in which *l* is written as:

$$l = \frac{L_3}{2n} \tag{2.66}$$

The relation between relative position of lumped mass x_i and the mass distance parameter *l* is written as:

$$x_i = (2i-1)l \qquad i = 1,...,n \tag{2.67}$$

Recalling the transverse displacement function *v*(*x*,*t*), position vector of an arbitrary lumped mass after deformation can be written in terms of local coordinate system.

$$\begin{aligned} \vec{r_i} &= (X\cos\theta_3 + Y\sin\theta_3 + (2i-1)l)\vec{i} \\ &+ (Y\cos\theta_3 - X\sin\theta_3 + v_i(x_i,t))\vec{j} \end{aligned} \tag{2.68}$$

where *X* and *Y* are given by Equations 2.43.b and 2.43.c, respectively.

In Equation 2.68, $v_i(x_i,t)$ represent the transverse displacement function of the i-th lumped mass. If two times derivation is taken with respect to time, acceleration expressions in *x* and *y* direction for a lumped mass can be written as:

$$\vec{a}_{xi} = -L_2\dot{\theta}_2^{\,2}\cos\theta_2\cos\theta_3 - L_2\dot{\theta}_2^{\,2}\sin\theta_2\sin\theta_3 - (2i-1)l\dot{\theta}_3^{\,2} - 2\dot{\theta}_3\dot{v}_i(x_i,t) - \ddot{\theta}_3 v_i(x_i,t) \quad (2.69)$$

$$\vec{a}_{yi} = L_2\dot{\theta}_2^{\,2}\cos\theta_2\sin\theta_3 - L_2\dot{\theta}_2^{\,2}\sin\theta_2\cos\theta_3 + (2i-1)l\ddot{\theta}_3 + \ddot{v}_i(x_i,t) - \dot{\theta}_3^{\,2} v_i(x_i,t) \quad (2.70)$$

Longitudinal and transverse inertia force components as D'Alembert forces that effect on the each lumped masses are given by the following equations:

$$\vec{D}_{xi} = -m_{3i}\,\vec{a}_{xi} \quad (2.71)$$

$$\vec{D}_{yi} = -m_{3i}\,\vec{a}_{yi} \quad (2.72)$$

For determining joint forces exerted on the coupler, it is necessary to write force and moment equilibrium conditions for coupler similar with the previous section. Instead of integral terms, discrete summations are used for lumped system. Joint forces at both ends, shown in Figure 2.5 and 2.6 are given below:

$$F_y^{\,43} = -\frac{1}{L_3}\sum_{i=1}^{n}(2i-1)lD_{yi} + \frac{1}{L_3}\sum_{i=1}^{n} v_i(x_i,t)D_{xi} \quad (2.73)$$

$$F_y^{\,23} = -F_y^{\,43} - \sum_{i=1}^{n} D_{yi} \quad (2.74)$$

$$F_x^{\,43} = F_y^{\,43}\cot\theta_3 + F_X^{\,43}\csc\theta_3 \quad (2.75)$$

$$F_x^{\,23} = -F_x^{\,43} - \sum_{i=1}^{n} D_{xi} \quad (2.76)$$

where $F_X^{\,43}$ is written as:

$$F_X^{43} = -M_4(L_2\omega_2^2\cos\theta_2 + L_3\dot{\theta}_3^2\cos\theta_3 + L_3\ddot{\theta}_3\sin\theta_3) \tag{2.77}$$

In order to obtain the right hand side of the Equation 2.61, it is required to express the bending moment function along the coupler. Bending moment expression can be written as:

$$M(x_i,t) = F_y^{23}(2i-1)l - F_x^{23}v_i(x_i,t) + \sum_{j=1}^{i}2(i-j)lD_{yj} - \sum_{j=1}^{i}\left(v_i(x_i,t) - v_j(x_j,t)\right)D_{xj} \tag{2.78}$$

If joint forces F_y^{23} and F_x^{23} are substituted into the bending moment expression given by Equation 2.78, the equation of motion for the lumped mass becomes:

$$\begin{aligned}
EI\frac{\partial^2 v(x,t)}{\partial x^2}\bigg|_{x=x_i} &= \sum_{j=1}^{i}\left[(2i-1)\frac{l}{L_3} - \frac{v_i(x_i,t)}{L_3}\cot\theta_3 - 1\right](2j-1)lD_{yj} \\
&+ \sum_{j=i+1}^{n}\left[\left((2j-1)\frac{l}{L_3} - 1\right)(2i-1)l - \frac{v_i(x_i,t)}{L_3}\cot\theta_3(2j-1)l\right]D_{yj} \\
&+ \sum_{j=1}^{i}\left[\left(1-(2i-1)\frac{l}{L_3}\right)v_j(x_j,t) + \frac{v_i(x_i,t)}{L_3}\cot\theta_3 v_j(x_j,t)\right]D_{xj} \\
&+ \sum_{j=i+1}^{n}\left[(2i-1)\frac{l}{L_3}v_j(x_j,t) - v_j(x_j,t)\frac{v_i(x_i,t)}{L_3}\cot\theta_3 + v_i(x_i,t)\right]D_{xj} \\
&+ v_i(x_i,t)\left(-M_4(L_2\omega_2^2\cos\theta_2 + L_3\dot{\theta}_3^2\cos\theta_3 + L_3\ddot{\theta}_3\sin\theta_3)\right)\csc\theta_3
\end{aligned} \tag{2.79}$$

This single equation is derived for only a single lumped mass located on the neutral axis of the flexible coupler. A set of equations for all masses on the link can be written for *i=1,2..n*. Equation 2.79 includes nonlinear terms due to the multiplication of transverse displacement function by itself or its derivatives. It is not easy to solve this nonlinear partial differential equation in this form.

Finite difference approximation is used for the derivation with respect to x, namely the coefficient of *EI* appeared in Equation 2.79. Therefore, the problem is reduced to solution of a set of ordinary differential equations with time derivatives which can be solved by any numerical methods.

2.4. Finite Difference Method for Dynamic Elastic Deflections

Numerical techniques are widely used to solve the boundary and initial value problems which come out in many fields of engineering. Finite difference method is one of the numerical techniques which frequently used and give effective and convenient solutions for differential equations. (Hildebrand 1987). The applicability of this method to complex geometries and the simplicity of solution procedure are the advantages of this method over other numerical techniques.

In Finite Difference Method, either ordinary or partial derivatives are replaced with finite difference formulas, so the differential equation which to be solved becomes algebraic set of equations that easy to deal with.

Considering a function $v(x, t)$ depends on two variables x and t, derivation of this function with respect to independent variables are replaced by finite difference approximations in partial differential equation. Hence, domain of the function is divided into sub-domains which constitute the meshes of the function. Mesh size can be uniform as well as nonuniform. Differential equation is enforced only at this mesh points and in our problem, it corresponds to points that lumped masses located. Thus, discrete values of function $v(x,t)$ is obtained. Discretization of space and time domain of a function is shown in Figure 2.9 with mesh points x_i and t_j.

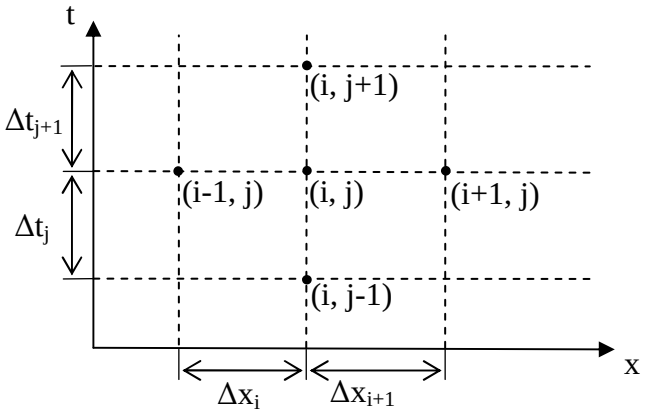

Figure 2.9 Discretization of functions with two variables.

To deal with our problem, the second derivative of $v(x,t)$ with respect to x is replaced with second order central difference formula. By writing Taylor series expansion of $v(x,t)$, about point x_{i-1}:

$$v(x_{i-1},t) \cong v(x_i,t) - \Delta x_i \left(\frac{\partial v(x,t)}{\partial x} \right)_i + \frac{1}{2} \Delta x_i^{\,2} \left(\frac{\partial^2 v(x,t)}{\partial x^2} \right)_i \tag{2.80}$$

Although, first three terms of the Taylor series expansion is written, it should be noted that a truncation error $O(\Delta x^2)$ is exist which will be ignored. If an expansion of $v(x,t)$ about point x_{i+1} is written:

$$v(x_{i+1},t) = v(x_i,t) + \Delta x_{i+1} \left(\frac{\partial v(x,t)}{\partial x} \right)_i + \frac{1}{2} (\Delta x_{i+1})^2 \left(\frac{\partial^2 v(x,t)}{\partial x^2} \right)_i \tag{2.81}$$

First derivative terms written in the expression are eliminate to give second derivation finite difference formulation:

$$\left(\frac{\partial^2 v}{\partial x^2} \right)_i = \frac{2[\Delta x_{i+1} v(x_{i-1},t) - (\Delta x_i + \Delta x_{i+1}) v(x_i,t) + \Delta x_i v(x_{i+1},t)]}{\Delta x_i \Delta x_{i+1} (\Delta x_i + \Delta x_{i+1})} \tag{2.82}$$

Equation 2.82 along with boundary conditions given by the Equations 2.63 and 2.64 are substituted into Equation 2.79, to obtain a set of ordinary differential equations depend on time and time derivatives of unknown functions representing the transverse displacements of coupler at point x_i. The set of equations found using the procedure outlined above are written as follows:

$$\begin{aligned}
&\frac{EI}{l^2} \left(-v_1(t) + \frac{1}{3} v_2(t) \right) = M(x_i,t) && i = 1 \\
&\frac{EI}{4l^2} \left(v_{i-1}(t) - \frac{1}{2} v_i(t) + v_{i+1}(t) \right) = M(x_i,t) && i = 2,\ldots, n\text{-}1 \\
&\frac{EI}{l^2} \left(\frac{1}{3} v_{n-1}(t) - v_n(t) \right) = M(x_i,t) && i = n
\end{aligned} \tag{2.83}$$

where $M(x_i,t)$ is given by Equation 2.78.

A symbolic mathematical program based on Equation 2.78 is developed to solve the equations of motion to achieve the dynamic responses of the system for the initial conditions given below:

$$v_i(0) = 0 \qquad i = 1,\ldots, n \tag{2.84}$$

$$\dot{v}_i(0) = 0 \qquad i = 1,\ldots, n \tag{2.85}$$

CHAPTER 3

NUMERICAL RESULTS AND DISCUSSION

3.1. Introduction

In this chapter, using the developed program tested by the results available in the literature (Sadler and Sandor 1973), dynamic responses for the midpoint of the flexible coupler are presented with respect to crank angle for different mechanism properties. The parameters that effect the elastic deflections of the flexible links are discussed.

3.2. Verification of Developed Program

Developed program based on the Equation 2.83 is tested by using the results given by (Sadler and Sandor 1973). The excellent agreement has been found between the present results and the results of the aforementioned study.

3.3. Dynamic Responses of Slider-Crank Mechanism

3.3.1. Dynamic Response of the Example Mechanism

In this subsection, elastic deflection results are given for a slider-crank mechanism shown in the Figure 3.1. Numerical values belong the example mechanism are also listed below:

$L_3 = 0.3048\ m$	Coupler length
$L_2 = 0.5\ L_3$	Relation between crank and coupler lengths
$M_4 = 0.25\ M_3$	Relation between slider and coupler masses
$E = 6.9 \times 10^{10}\ N/m^2$	Modulus of elasticity of coupler
$\rho = 2770\ kg/m^3$	Density

$b = 0.0254\ m$	Width of the cross-section of the coupler
$h = 0.00206\ m$	Height of the cross-section of the coupler
$\omega_2 = 50\ rad/s$	Operation speed of the rigid crank

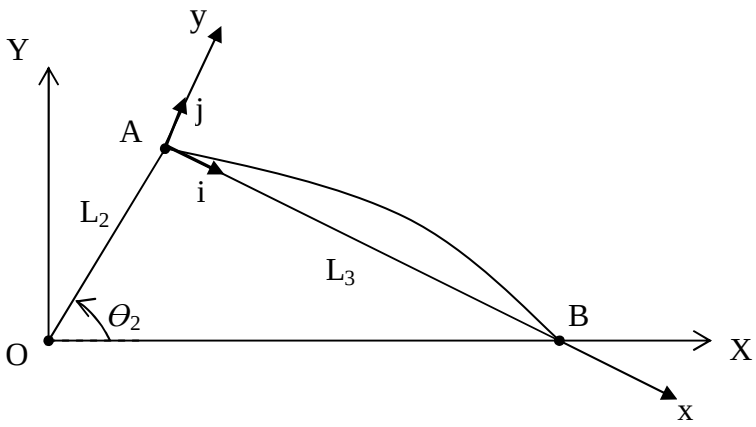

Figure 3.1. Mechanism with significant properties

Elastic deflection of the midpoint of coupler versus time plot is given for two cycles of the crank in Figure 3.2. It is clear that, if the horizontal axis of the plot is changed to crank angle, the same graph is obtained.

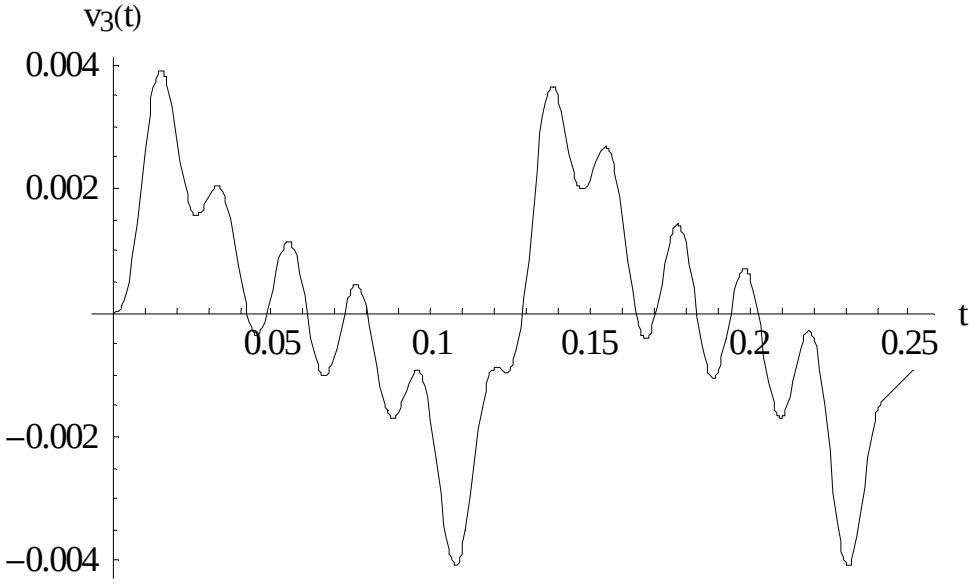

Figure 3.2. Elastic deflections of the midpoint of coupler

3.3.2. Effects of the Link Masses on Dynamic Responses

Link masses are one of the design parameters that should be interested. While obtaining the dynamic response of the flexible coupler, masses of slider and coupler are effective on result. To see this effect, considering the mass of the coupler as in the example mechanism, three selected slider mass depending on the mass ratios between the coupler and slider are given as:

$$\left(\frac{M_4}{M_3}\right)_1 = 0.10 \quad , \quad \left(\frac{M_4}{M_3}\right)_2 = 0.25 \quad , \quad \left(\frac{M_4}{M_3}\right)_3 = 0.50 \tag{3.1}$$

Other parameters are selected as the same with the example mechanism. The results of three different cases for two cycles of crank rotation are given in Figure 3.3 together.

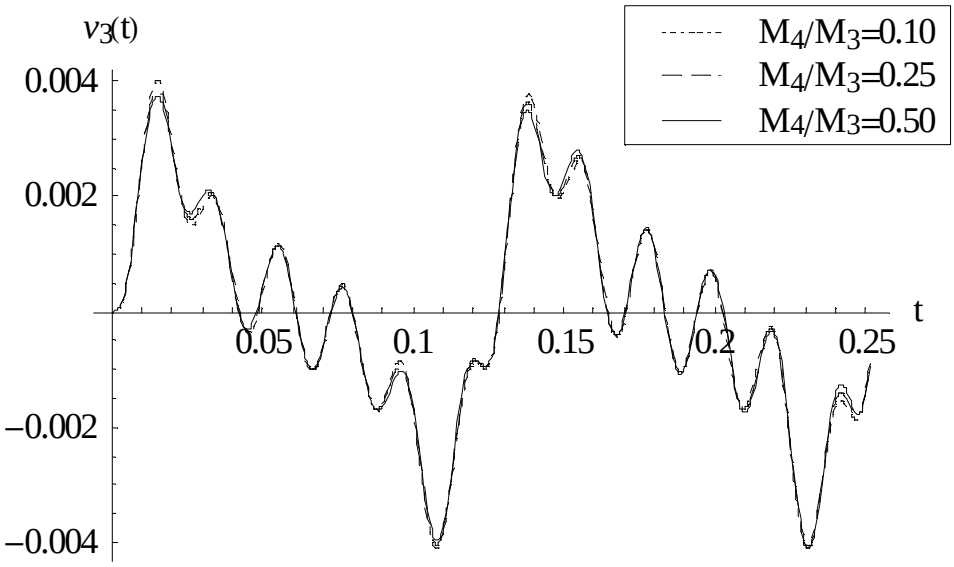

Figure 3.3. Elastic deflections for various mass properties

It can be seen from Figure 3.3 that mass of the slider does not affect the deflection of the coupler excessively.

3.3.3. Effects of the Operation Speeds on Dynamic Responses

It is obvious that operation speeds have a significant role on elastic behaviors of flexible linkages. High operation speeds generates high deflections on the coupler. It can be seen by considering different rotation speeds for crank as, ω_2=40 *rad/s*, ω_2=50 *rad/s*, ω_2=60 *rad/s*.

Dynamic displacement of midpoint of the coupler for M_4/M_3=0.10 is plotted for two cycles of crank rotation in Figure 3.4

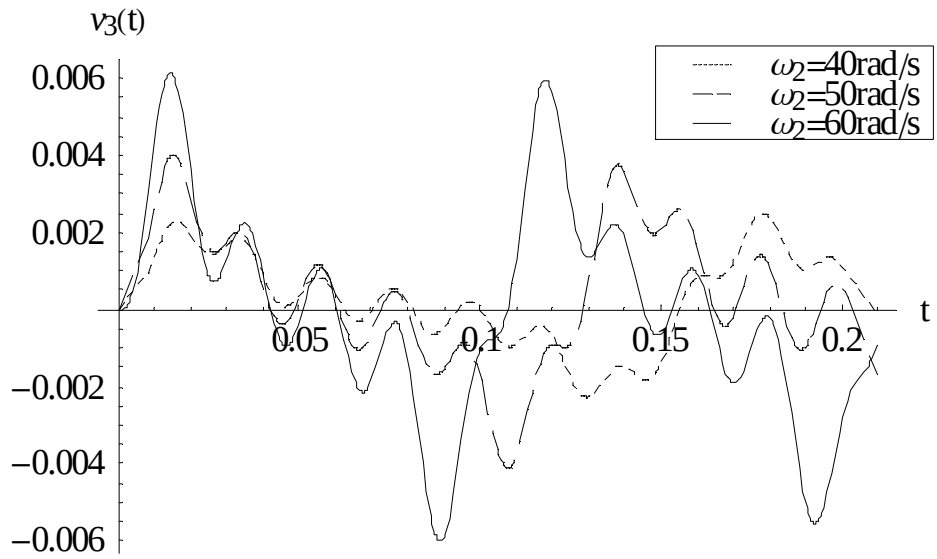

Figure 3.4. Effects of operation speed on elastic behavior for mass ratio 0.10

It can be seen from Figure 3.4 that the absolute values of the elastic deflections of the coupler increase, when the angular velocity of crank increases. Therefore, it is necessary to choose lower speed values if it is feasible in mechanism systems. However, high-operated systems are indispensable mostly in modern machinery. So, it is essential to investigate the effects of operation speed on dynamic response with other parameters.

To examine the effect of crank rotation on the elastic deflection of coupler, the different mass ratios for between the coupler and slider can be chosen.

Dynamic displacement of midpoint of the coupler for M_4/M_3=0.25 and M_4/M_3=0.50 are plotted for two cycles of crank rotation in Figures 3.5 and 3.6, respectively.

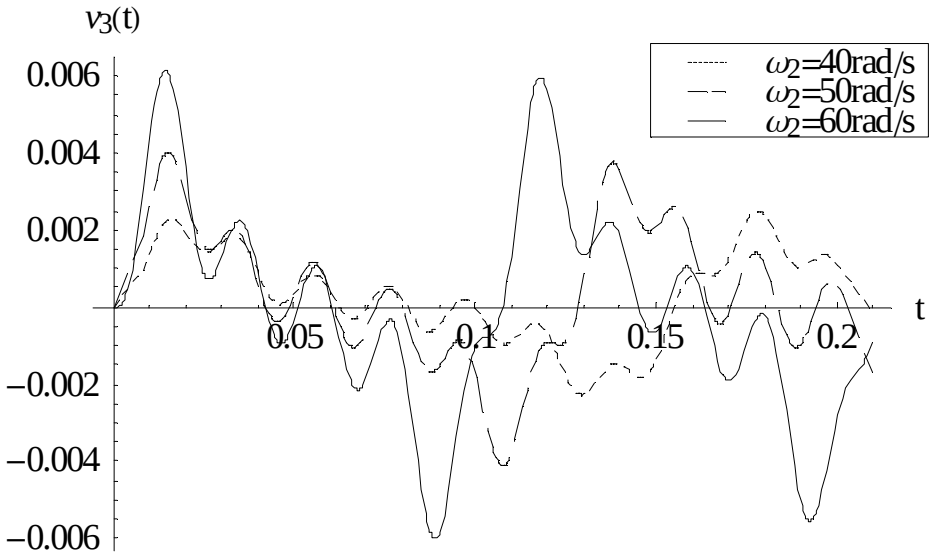

Figure 3.5. Effects of operation speed on elastic behavior for mass ratio 0.25

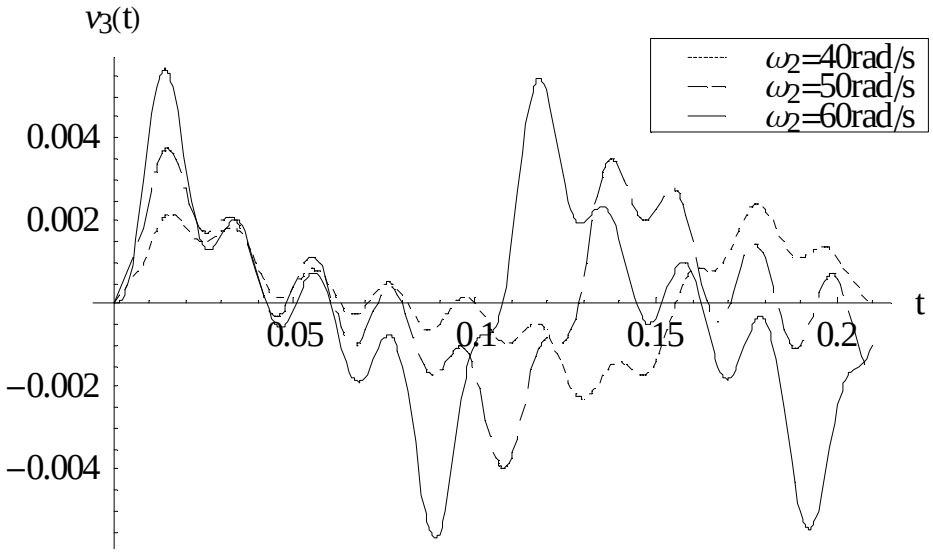

Figure 3.6. Effects of operation speed on elastic behavior for mass ratio 0.50

It can be seen from Figures 3.5 and 3.6 that the same tendency in the Figure 3.4 is observed.

It can also be seen that from the Figures 3.4, 3.5, and 3.6 that the two cycles of crank rotation is completed just for the response plotted for ω_2=60 *rad/s*. Other responses have some delays to complete their two periods.

3.3.4. Effects of the Crank Length on Dynamic Responses

To see the effects of the length ratio between the crank and coupler on the dynamic response; while the length of the coupler L_3 is taken as in the example mechanism, three different length ratios given below are selected:

$$\left(\frac{L_2}{L_3}\right)_1 = 0.30 \qquad \left(\frac{L_2}{L_3}\right)_2 = 0.40 \qquad \left(\frac{L_2}{L_3}\right)_3 = 0.50 \tag{3.2}$$

In addition to the selection of different length ratios, three different operation speeds are also chosen to obtain their effects on dynamic response.

Dynamic displacement of midpoint of the coupler having the mass ratio M_4/M_3=0.1 for ω_2=40 *rad/s*, ω_2=50 *rad/s*, ω_2=60 *rad/s* are plotted for two cycles of crank rotation in Figures 3.7, 3.8, and 3.9, respectively.

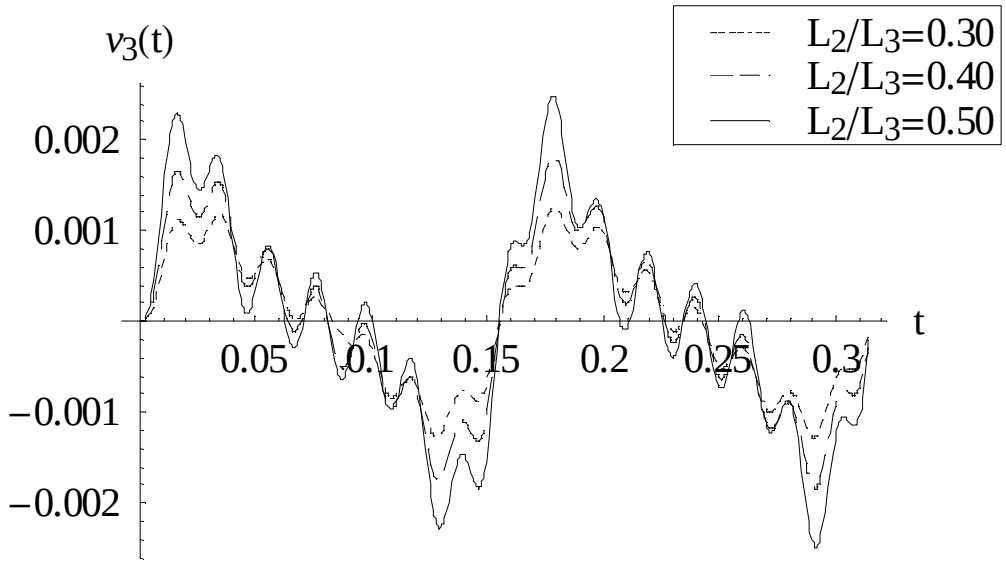

Figure 3.7. Effect of crank length for ω_2=40 *rad/s* and mass ratio 0.10

It can be seen from Figure 3.7 that the absolute values of the elastic deflections of the coupler increase, when the length ratio between the crank and coupler increases. Therefore, it is necessary to choose short crank length values if it is feasible in mechanism systems.

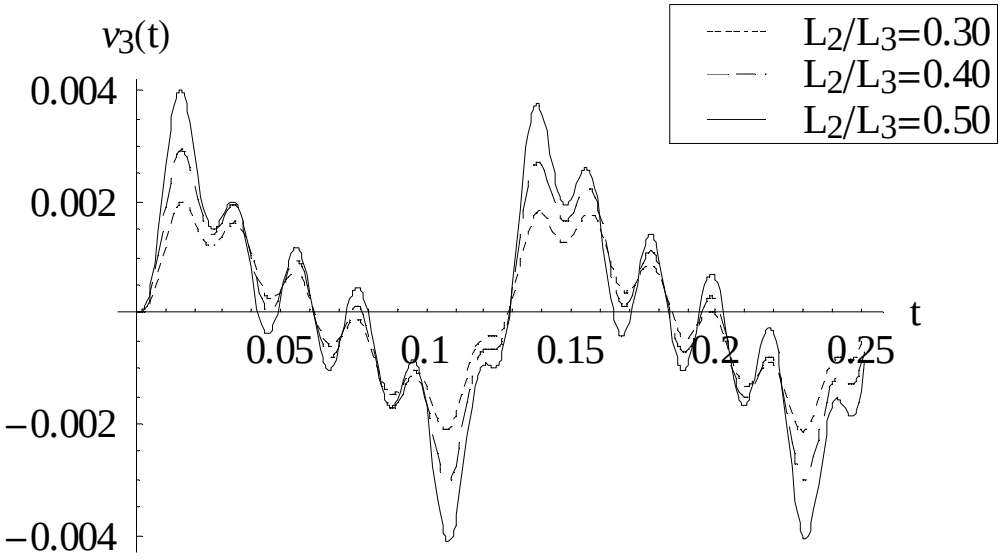

Figure 3.8. Effect of crank length for ω_2=50 *rad/s* and mass ratio 0.10

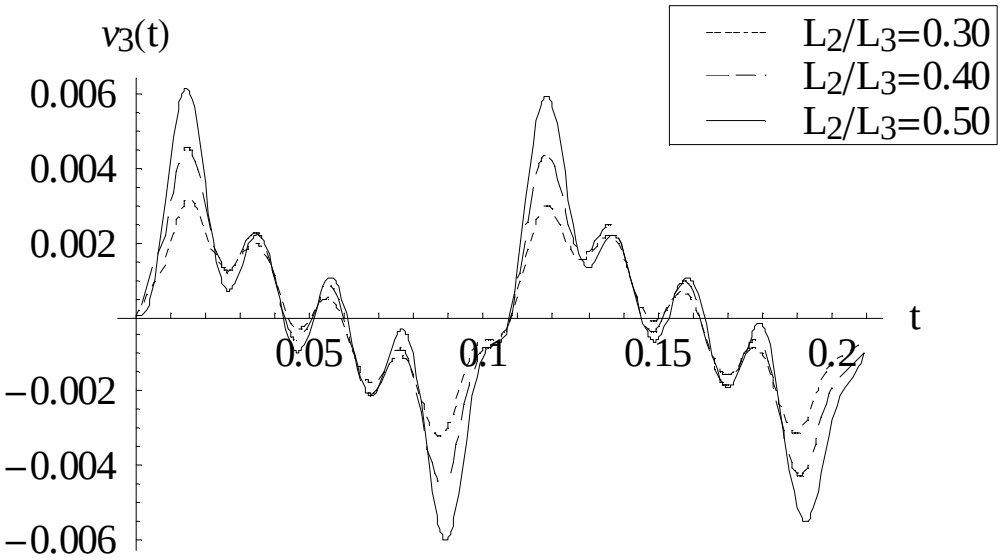

Figure 3.9. Effect of crank length for ω_2=60 *rad/s* and mass ratio 0.10

It can be seen from Figures 3.8 and 3.9 that the same tendency in the Figure 3.7 is observed.

Effects of the operation speeds on dynamic responses obtained and discussed in Section 3.3.3 can also be seen from the Figures 3.7, 3.8, and 3.9 that when the operation speed increase, the absolute values of the elastic deflections of the coupler increase.

Additionally, dynamic displacement of midpoint of the coupler having the mass ratio M_4/M_3=0.25 for ω_2=40 *rad/s*, ω_2=50 *rad/s*, ω_2=60 *rad/s* are plotted for two cycles of crank rotation in Figures 3.10, 3.11, and 3.12, respectively.

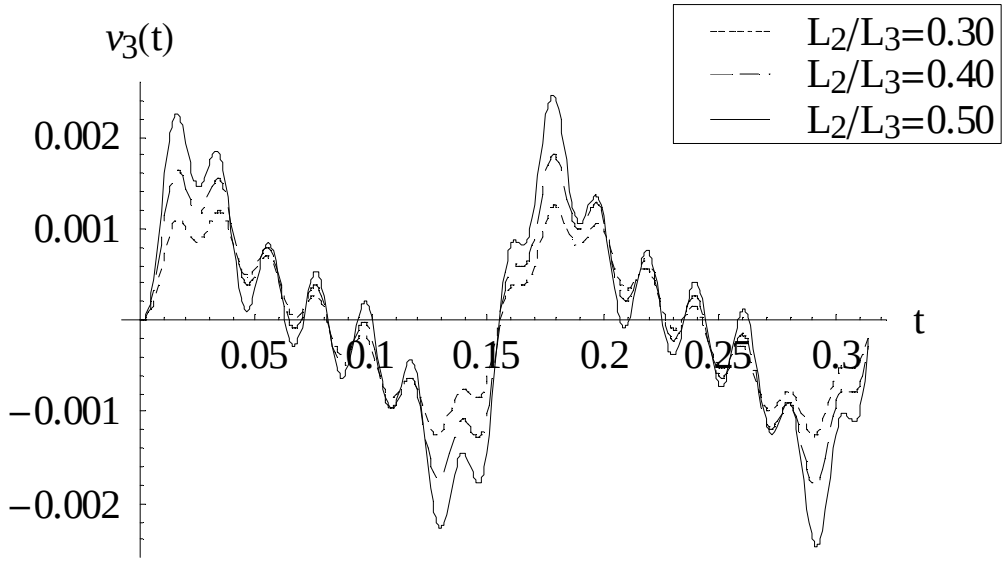

Figure 3.10. Effect of crank length for ω_2=40 *rad/s* and mass ratio 0.25

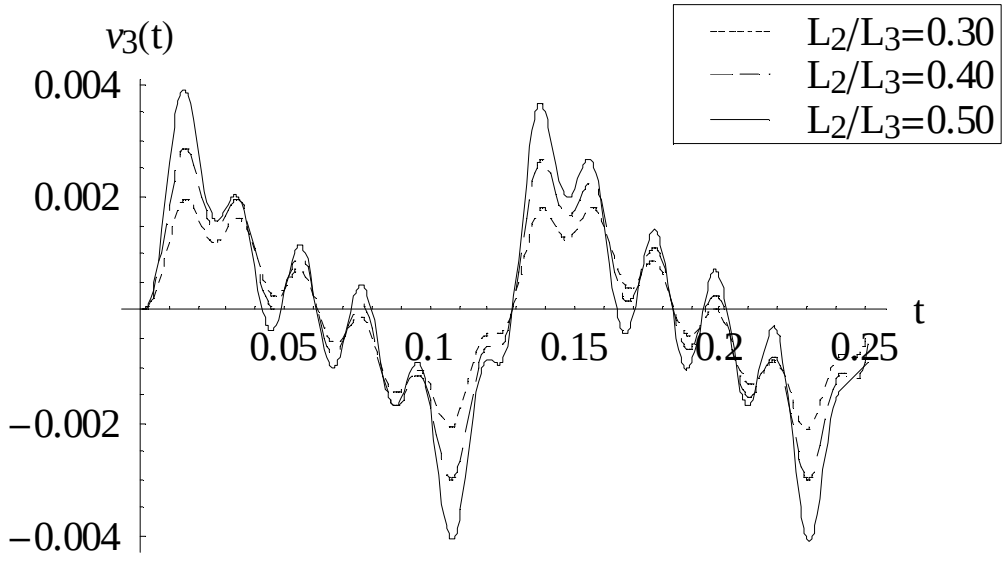

Figure 3.11. Effect of crank length for ω_2=50 *rad/s* and mass ratio 0.25

It can be seen from Figures 3.10, 3.11, and 3.12 that the elastic deflections of the coupler have different plots depending on the selected parameters.

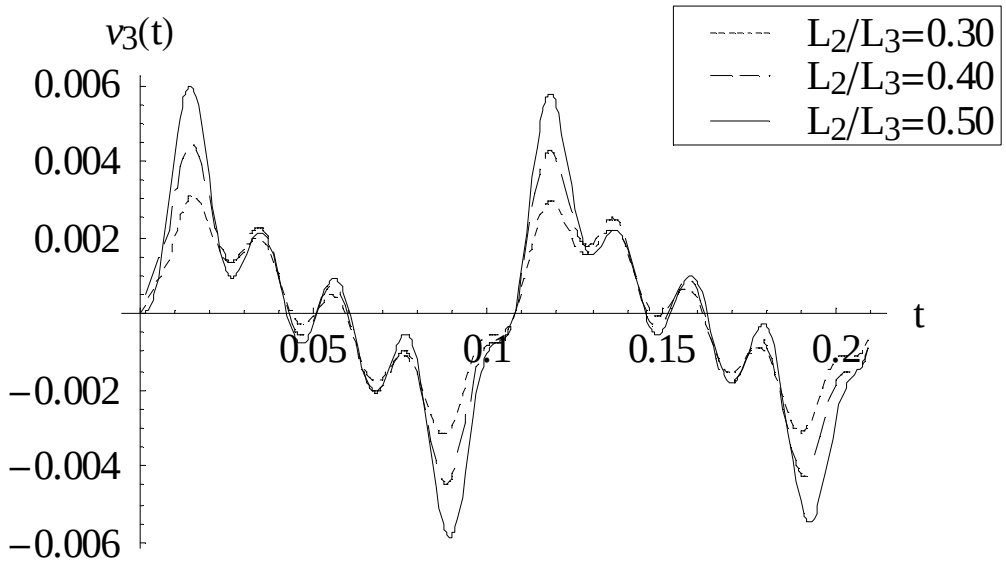

Figure 3.12. Effect of crank length for ω_2=60 *rad/s* and mass ratio 0.25

Furthermore, dynamic displacement of midpoint of the coupler having the mass ratio M_4/M_3=0.50 for ω_2=40 *rad/s*, ω_2=50 *rad/s*, ω_2=60 *rad/s* are plotted for two cycles of crank rotation in Figures 3.13, 3.14, and 3.15, respectively.

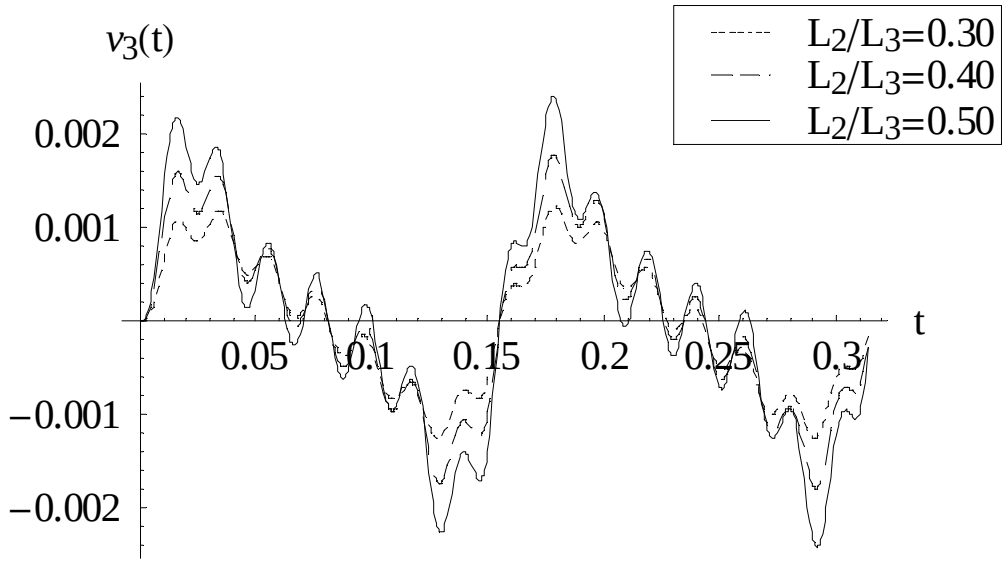

Figure 3.13. Effect of crank length for ω_2=40 *rad/s* and mass ratio 0.50

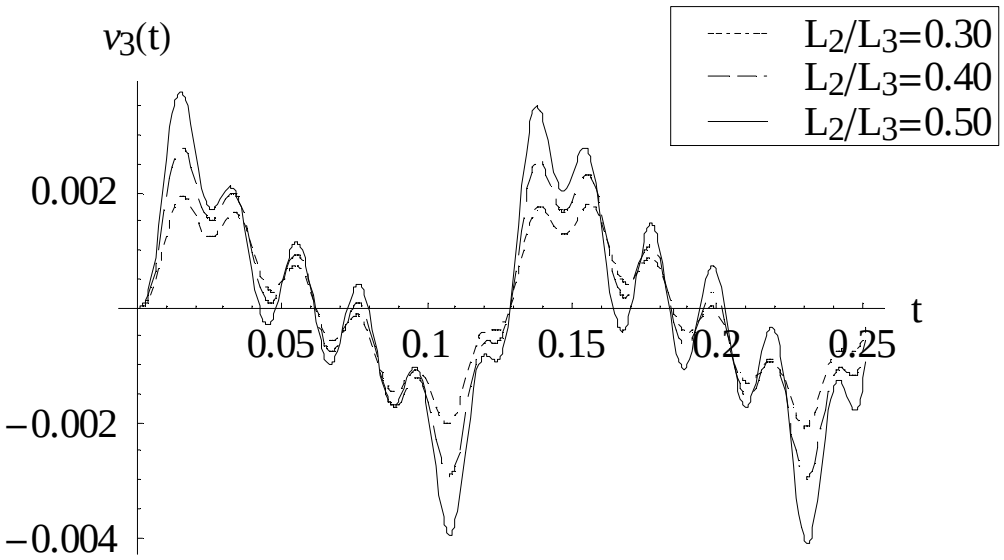

Figure 3.14. Effect of crank length for ω_2=50 *rad/s* and mass ratio 0.50

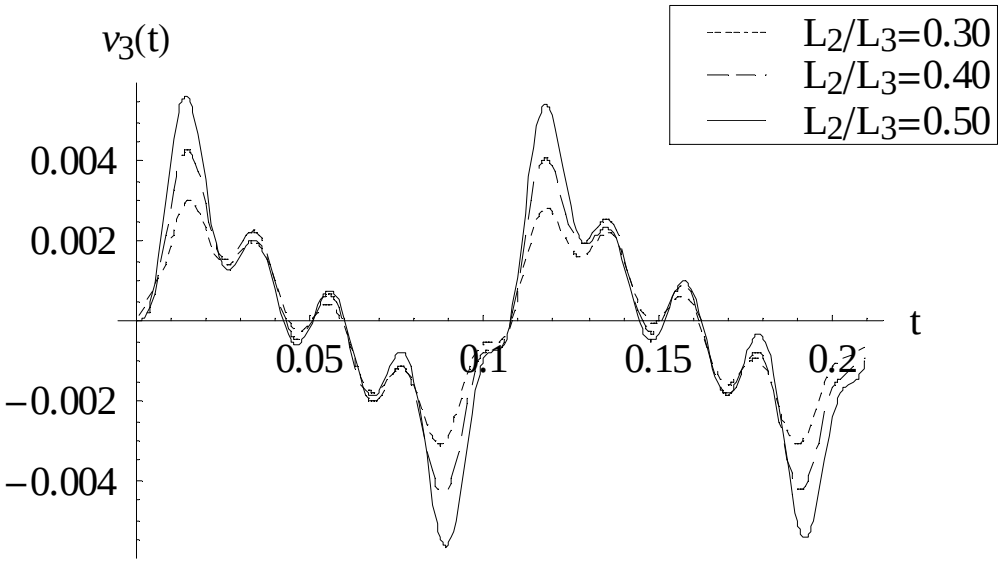

Figure 3.15. Effect of crank length for ω_2=60 *rad/s* and mass ratio 0.50

Similar to Figures 3.10, 3.11, and 3.12, Figures 3.13, 3.14, and 3.15 show that the elastic deflections of the coupler have different plots depending on the selected parameters.

CHAPTER 4

CONCLUSIONS

This study presents a solution procedure for the dynamic response of elastic linkages in mechanisms by using lumped parameter method. Slider-crank mechanism is chosen for this analysis since it is widely used in many industrial areas. Crank is assumed as rigid and the coupler is considered as flexible. This approach gives efficient solutions when it is compared to other studies available in the literature.

The applications of this mechanism with different design parameters are presented. The effects of these parameters such as crank length ratio, mass ratio, and operation speed on elastic behaviors of the mechanism are examined. The results and discussions are given in previous chapter.

REFERENCES

Chen, J. and C. Chian. 2001. Effects of crank length on the dynamics behavior of a flexible connecting rod. *Asme Journal of Vibration and Acoustics 123:318-323.*

De Jalon, J.G. and E. Bayo. 1993. *Kinematic and dynamic simulations of multibody systems*. Springer.

Fanghella, P., C. Galletti and G. Torre. 2003. An explicit independent-coordinate formulation for the equations of motion of flexible multibody systems. *Mechanism and Machine Theory 38:417-437.*

Fung, R. 1997. Dynamic responses of the flexible connecting rod of a slider-crank mechanism with time dependent boundary effect. *Computers and Structures 63(1):79-90.*

Hildebrand, F.B. (1987). Introduction to Numerical Analysis. New York, Dover Publications.

Karkoub, M. and A.S. Yigit. 1999. Vibration control of a four-bar mechanism with a flexible coupler. *Journal of Sound and Vibration* 222(2):171-189.

Sadler, J.P. and G.N. Sandor. 1973. A Lumped Parameter Approach to Vibration and stress analysis of elastic linkages. *ASME Journal of Engineering for Industry 95(2):549-557.*

Sadler, J.P. and G.N. Sandor. 1974. Nonlinear vibration analysis of elastic four-bar linkages. *ASME Journal of Engineering for Industry 96(2):411-419.*

Sadler, J.P. 1975. On the analytical lumped-mass model of an elastic four-bar mechanism. *ASME Journal of Engineering for Industry 97(2):561-565.*

Shabana, A.A. 2005. *Dynamics of multibody systems*. Cambridge University Press.

Söylemez, Eres. 1999. *Mechanisms.* METU, Publication Number:64

Turhan, Ö. 1993. Elastik biyelli üç-çubuk ve krank-biyel mekanizmalarının dinamik kararlılığı. *6. Ulusal Makina Teorisi Sempozyumu :385-399.*

Viscomi, B.V. and R.S. Ayre. 1971. Nonlinear dynamic response of elastic slider-crank mechanism. *ASME Journal of Engineering for Industry 93(1):251-262.*

Yang, K. and Y. Park. 1998. Dynamic stability analysis of a flexible four-bar mechanism and its experimental investigation. *Mechanism and Machine Theory 33(3):307-320.*

Yu, S.D. and W.L. Cleghorn. 2002. Dynamic instability analysis of high-speed flexible four-bar mechanisms. *Mechanism and Machine Theory 37:1261-1285.*

Yu, S.D. and F. Xi. 2003. Free vibration analysis of planar flexible mechanisms. Asme *Journal of Mechanical Design 125:764-772*.